Bar-Ilan University

Tunneling Measurements in Disordered Films near The Superconductor - Insulator Transition

Oriya Eizzenberg

Submitted in partial fulfillment of the requirements for the Master's Degree

In the Department of physics, Bar Ilan University.

Ramat-Gan, Israel 2017

Bar-Ilan University

Tunneling Measurements in Disordered Films near The Superconductor - Insulator Transition

Oriya Eizzenberg

Submitted in partial fulfillment of the requirements for the Master's Degree

In the Department of physics, Bar Ilan University.

Ramat-Gan, Israel 2017

This work was carried out under the supervision of

Prof. Aviad Frydman

Department of Physics, Bar-Ilan University.

Table of content

Abstract

The Superconductor-Insulator Transition (SIT) in thin films is a phenomenon which is in the front of condensed matter research today. It is considered a classical example of a quantum phase transition in which a system transits from an insulating state to a superconducting state at zero temperature. Most of the SIT research focuses on the "quantum critical regime", since in this regime the behavior of the films is non-trivial. Though this topic has generated a large research effort, both experimental and theoretical, much of the physics is not well understood.

One of the proposed models to explain some of the features observed in these systems is the “emergent granularity” model, which invokes the presence of granular behavior despite the fact that the films exhibit continuous morphology. Experiments have shown that this granularity is manifested by superconducting islands surrounded by an insulating sea. InO_x films, which undergo the SIT, are one example for this unique type of systems.

A good way to characterize any superconductor is by performing tunneling experiments to measure the density of states (DOS) which provides information on the energy gap, Δ, of the superconductor. Such measurement on highly disordered superconductors in the past have revealed the presence of superconductivity in the insulating phase.

In this work we measured the DOS of InO_x films close to the superconductor-insulator transition (SIT) with different disorder and various temperature. In clean superconductors the measured DOS fits the well-known BCS expression. On the other hand, the DOS of superconductors close to the SIT does not fit BCS. In particular, the coherence peaks at the gap edges are considerably suppressed.

We used a new approach to analyze the tunneling data. This approach takes into consideration the electronic structure (emergent granularity) in which Δ is not a constant but a bosonic field that fluctuates in space and time $\{\Delta(r,t)\}$. One can express Δ as a combination on effects of long range and short range correlations: We analyze our data using this model and find that it fits the results much better than BCS by adding just one fitting parameter.

The main conclusions from the analysis of the data are:

1. Δ does not change with disorder and temperature. Moreover, it stays rather constant even above T_c and in the insulator.
2. Near the SIT the BCS theory is not enough to describe the physics. We show that fluctuations of the superconducting order parameter must be taken into consideration in order to understand the physics.
3. The need for new approach grows as the system approaches the SIT.

1.Introduction

1.1 QPT- quantum phase transitions

A classical phase transition is governed by thermal fluctuations and is characterized by a critical temperature, above which the system is in one phase, and below it – the system transits to another phase. An example for a second order phase transition is superconductivity, in which the system transits from a normal state to a superconducting state at a critical temperature, T_c. In recent years, there is a lot of interest in a different type of phase transition, a quantum-phase transitions [1-2] (QPT). Unlike thermal phase transitions that are governed by thermal fluctuations, a QPT is controlled by quantum fluctuations at $T = 0$ as a function of a tuning parameter, g, which is non-thermal. At $T = 0$, the phase transition occurs from one phase to the other at a quantum critical point (QCP), $g = g_c$, while at $T > 0$, a quantum critical region is generated around g_c, as sketched in fig. 1.1.

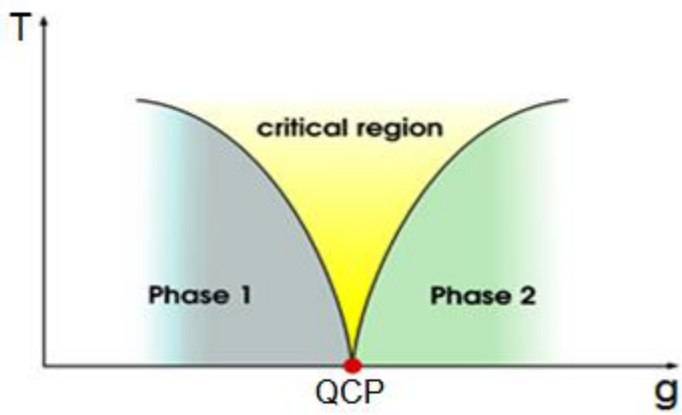

Fig. 1.1. An illustration of a quantum phase transition as a function of a tuning parameter g, where g_c is the critical point $T = 0$. At $T > 0$, there is a quantum critical region with a temperature dependent width.

In the quantum critical region, the system is neither in phase one, nor in the other rather, there are quantum fluctuations of one phase in the other. This is the most interesting area which will be the main focus of this work.

1.2 SIT – superconductor to insulator transition

Prototype QPT is the SIT (superconductor to insulator transition). The phenomenon of superconductivity is well understood in a perfect crystal (i.e. in the absence of impurities) thanks to the work of Bardeen, Schrieffer, and Cooper (BCS) [3]. They established the most common theory of superconductivity by identifying the mechanism of effective attraction between electrons mediated the phonon coupling. Due to this attraction, the electrons form Cooper pairs, whose condensate is a macroscopic superconducting state. Following BCS, Anderson [4] predicted that the superconducting phase can exist even in the presence of (nonmagnetic) impurities. This was found to be true in weak disorder. However experiment showed that for strong disorder the system transits from superconductivity to an insulator state. Anderson's theorem initiated the investigation of disordered superconductors, the interplay between disorder and superconductivity being one of the hottest topics in the current study of condensed matter. Thin films became a matter of great interest in the context of the possibility to observe a superconductor to insulator transition [5-8]. Experimentally a wide variety of tuning parameters g was used: thickness, magnetic field, disorder level, chemical structure, etc[9-11]. An example for an SIT that depends on the level of disorder can be seen in fig. 1.2 that presents transport measurements in two samples of thin amorphous indium oxide (InO_x) with different level of disorder, one sample is a superconductor and the other is an insulator.

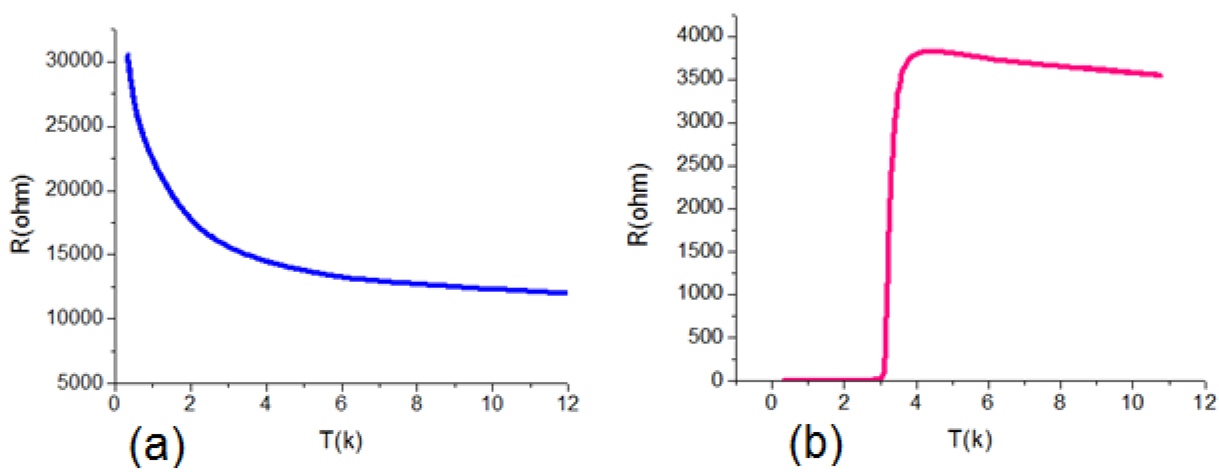

Fig. 1.2: R(T) of two different films of InO_x having different disorder level (controlled by thermal annealing) one is an insulator (a) and the other a superconductor (b).

1.3 Different types of SIT

The superconductor wave function is given by the expression: $\Psi = \Psi_0 e^{i\theta}$. Ψ_0- represents the amplitude and θ represents the phase. Hence, Superconductivity requires both finite amplitude and phase coherence throughout the sample. The amplitude depends on the density of Cooper pairs while the phase depends on the coupling between all parts of the system. Disorder in the system can influence both these parameters and therefore, the superconductivity can be suppressed either by phase fluctuations or by Cooper pairs fluctuations. Disordered films can be roughly categorized into two groups: granular and homogeneous. Fig. 1.3 shows transport measurements in two types of tin (Sn) films as a function of thickness. In both cases thin samples are insulators and thicker samples are superconducting, however the SIT is very different: while in homogeneous Sn there is a well-defined T_c which rises with growing thickness, in granular Sn T_c is not very well defined because the resistances don't drop sharply to zero. However there is a mark of T_c bulk – in all layers the resistance shows a change at $T = 4.3k$. In all the graphs of granular Sn the resistance starts to drop at the same temperature. The two behaviors represent two models of the SIT as discussed in the following paragraphs.

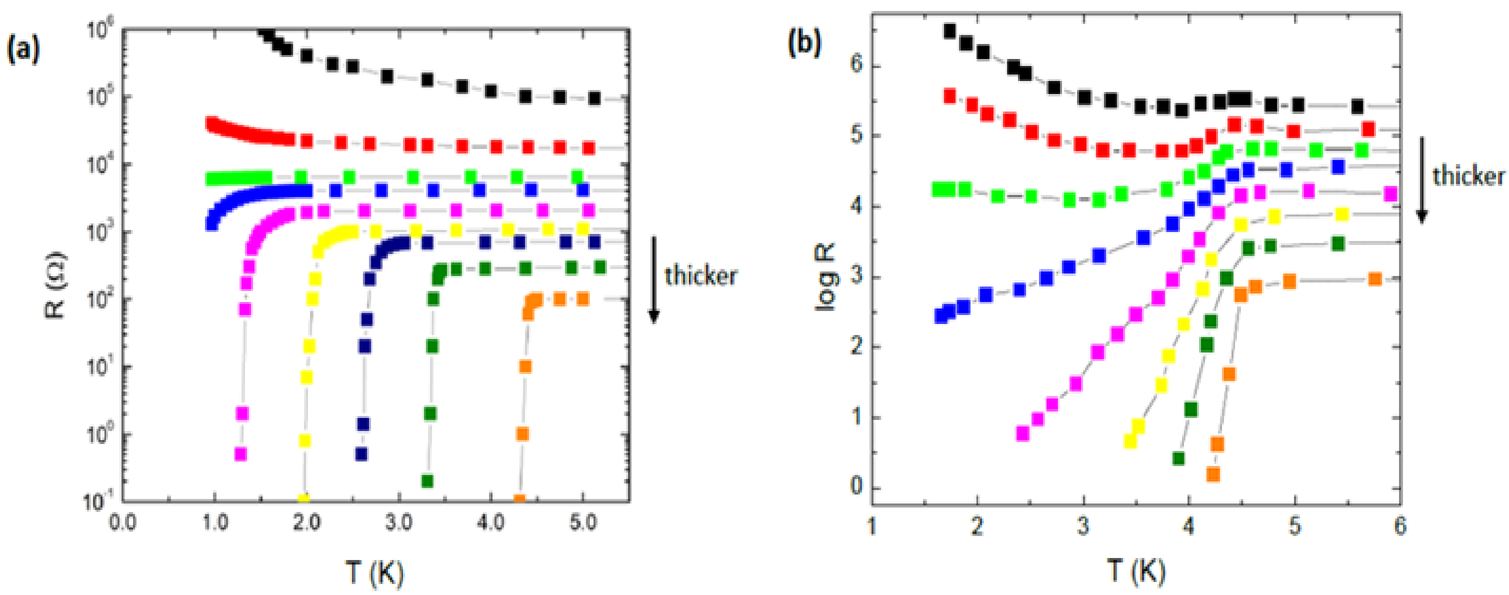

Fig. 1.3. (a) R(T) of homogeneous Sn as a function of thickness, in this case T_c grows as a function of thickness. (b) R(T) of granular films: note the change in the behavior in T=4.3k, reproduced from[12].

1.4 Fermionic model (homogeneous films)

One model for SIN was suggested by Finkelshtein [13]. In homogeneous films the phase is constant and the disorder in the system leads to Anderson localization [14]. Localization of electrons suppresses the electronic screening and this prevents electron-electron attraction. Therefore, the main effect of disorder is to decrease the density of Cooper pairs resulting in a decrease of T_c. In this model the system is insulating because of the localization of electrons, hence it is called the fermionic model.

The dimensionality of the system strongly influences the effect of the disorder. In three dimensions, the influence of impurities is smaller because of the large number of paths in the sample. In two dimensions, the disorder is a more significant parameter because there are much less options for the electron to transfer from one side to the other. When the thickness of the samples is increased, the effects of disorder decreases, thus increasing T_C .This naturally accounts for fig. 1.3a.

1.5 Bosonic model (Granular films)

The second model for SIT was suggested by Fisher [15], for which a representing sample is a granular film: The SIT in granular films can be explained by the presence of grains which are potential barriers for the electrons, thus localizing the wave function and the energy levels of the electrons. Despite the fact that every grain can be a perfect superconductor, there is no superconductivity throughout the sample because the grains do not communicate. As a result, the destruction of superconductivity is caused by fluctuations in the phase (θ). In these films there are two types of T_c.

1. T_c^{pb}: A local T_c for every grain – this is the temperature of pair braking.
2. T_c^{θ}: Macroscopic T_c $(\text{for which } R = 0)$ – is the temperature of phase coherence throughout the entire sample.

Fig. 1.3b shows that the T_c^{pb} does not change with thickness because the density of Cooper pairs does not change. On the other hand, T_c^{θ} changes as a function of the thickness: As the film thickness increase there are more areas of phase coherence in the sample. In this model the system is insulating because the Cooper pairs are localized on grains, which is why it is called the bosonic model.

In summary: in homogeneous films, destruction of the superconductivity is caused by the Cooper pair breaking. In granular films, destruction of the superconductivity is caused by phase incoherence between the grains.

1.6 Emerging electronic granularity

A third type of SIT systems appears in structurally homogeneous films that show properties of electronic granularity. An example for such a system is a thin film of InO_X. Despite the fact that the sample is homogeneous, it shows signs of granularity, such as signs of superconductivity even in the insulator. One important example for this is the behavior of the density of states (DOS) through the SIT. In the following paragraph we describe the DOS in a clean superconductor versus the DOS in a system close to the SIT.

1.7 Density of states

A major characteristic of the BCS theory is the unique DOS of a superconductor. While in a metal, the DOS is constant around the Fermi level, in superconductors the DOS is described by the formula:

$$\mathrm{N(E)_{BCS}} = \left|\mathrm{Re}\left[\frac{\mathrm{E}}{\sqrt{\mathrm{E^2} - \Delta(\mathrm{T})^2}}\right]\right| \tag{1.2}$$

Eq. 1.2 reveals that there is an energy gap of $\pm\Delta$ around the Fermi level, followed by a discontinues jump in the DOS. At high energies the DOS approaches the normal state value as seen in fig. 1.4.

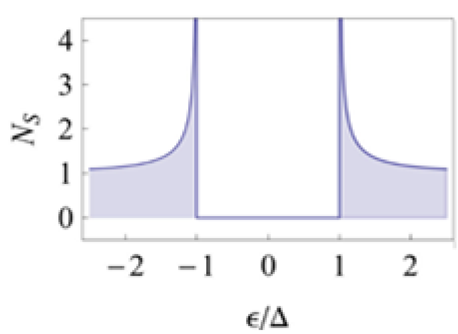

Fig. 1.4: DOS for a BCS superconductor at $\mathrm{T} = 0$. When $\mathrm{E} < \Delta$ there are no states $(\mathrm{N} = 0)$ and at $\mathrm{E} = \Delta$ there is a sharp jump in the DOS.

$\Delta(\mathrm{T})$ in eq. 1.2 is given by the BCS relation:

$$\Delta(\mathrm{T}) \sim \mathrm{T_C}\sqrt{1-\left(\frac{\mathrm{T}}{\mathrm{T_C}}\right)} \quad (1.3)$$

Fig. 1.5 shows a nice fit between eq. 1.3 to the measurements of $\Delta(\mathrm{T})$ in Niobium, Tantalum and Tin [16].

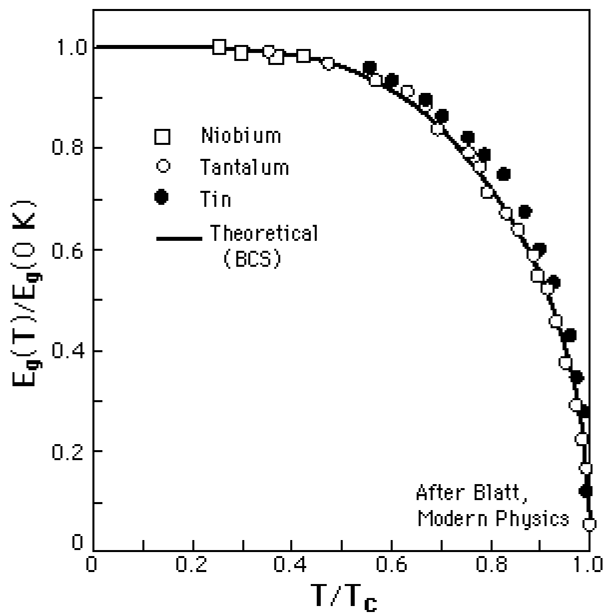

Fig. 1.5: Graph of $\frac{\Delta}{\Delta(\mathrm{T}=0)}$ as a function of $\frac{\mathrm{T}}{\mathrm{T_C}}$. The theoretical plot clearly shows that at $\mathrm{T} = \mathrm{T_c}$ $\Delta = 0$. The measurements of Δ in Niobium, Tantalum and Tin fit very well the BCS theory [16].

1.8 **DOS measurements**

Experimentally, the most effective way to measure the DOS is by tunneling experiments. A simple way to perform these measurements is to fabricate a superconductor- insulator – normal metal (SIN) junction as shown in Fig. 1.6. This setup allows to measure the I-V characteristic of the junction in a quasi 4-probe geometry.

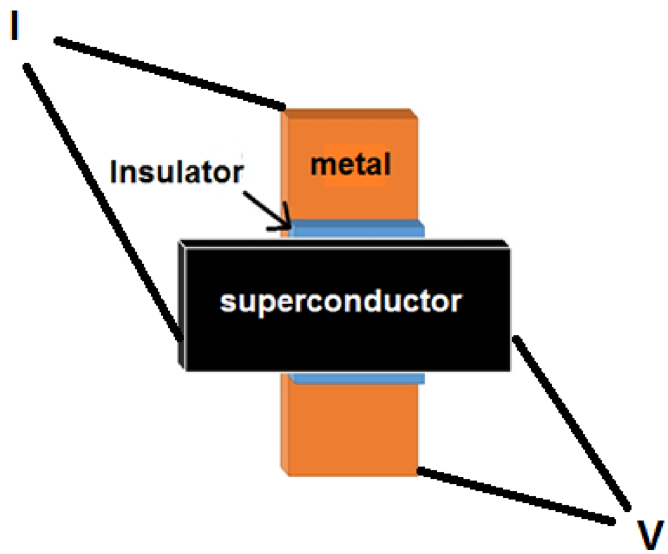

Fig. 1.6 Illustration of an SIN junction.

The tunneling probability depends on the DOS at both sides of the junction (N_2 , N_1):

$$P \sim N_1 * N_2 \tag{1.4}$$

Tunneling requires the presence of an electron on one side of the junction and a hole on the other. Because the DOS in metal is constant it can be shown that the differential conductivity $\left(\frac{dI}{dV}\right)$ of the junction is proportional to the DOS of the superconductor.

$$\left.\frac{dI}{dV}\right|_{T=0} \propto N_S(E) \tag{1.5}$$

When we substitute formula (1.2) into (1.5) we get the conductance through the junction:

$$\frac{dI}{dV} \Big/ \left[\frac{dI}{dV}(\text{normal})\right] = \left|(\text{Re}[\frac{E}{\sqrt{E^2 - \Delta(T)^2}}])\right| \tag{1.6}$$

In real systems there are thermal and electromagnetic noises, which cause smearing of $\frac{dI}{dV}$. Dynes [17] introduced a correction for the DOS and got the following formula:

$$G = \left|(\mathrm{Re}[\frac{E - i\Gamma}{\sqrt{(E-i\Gamma)^2 - \Delta(T)^2}}])\right| \tag{1.7}$$

Γ- is a phenomenological smearing parameter that takes into account all the thermal and electromagnetic noises. Experiments find a good agreement to eq. 1.7 as can be seen in fig. 1.7 that shows the comparison between the normalized measurements of $\frac{dI}{dV}$ in Aluminum at $T = 0.06K$ (dashed line) and the best fit to eq. 1.7.

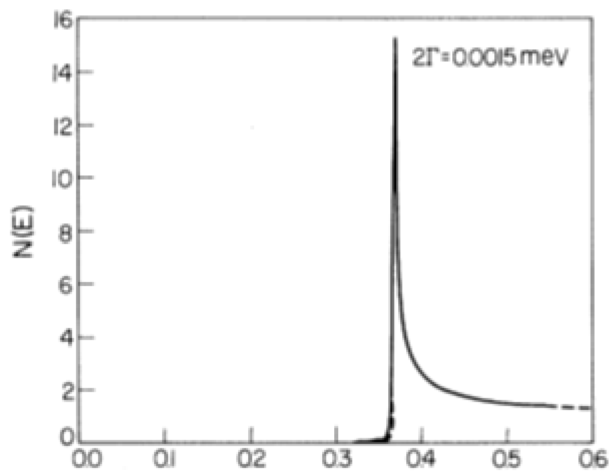

Fig. 1.7: Tunneling measurements on Aluminum. This measurements show a nice fit to eq. 1.7 [17].

1.9 DOS near the SIT

Measurements on films that are close to the SIT shown on fig. 1.8 [18]: Tunneling measurements in two different films of InO_X, with a fit to eq. 1.7. The first is a superconductor and the other is an insulator. Two important points can be deduced from this figure:

1. The DOS in the insulator and in the superconductor are very similar. The energy gap is the same although the coherence peaks at the gap edges are more suppressed in the insulator. The fact that a superconductor gap is seen in the insulator is consistent with electronic granularity that predicts superconductivity in the insulator.
2. The experiment does not fit eq. 1.7 very well. It is obvious that for highly disordered superconductors the theory should be corrected.

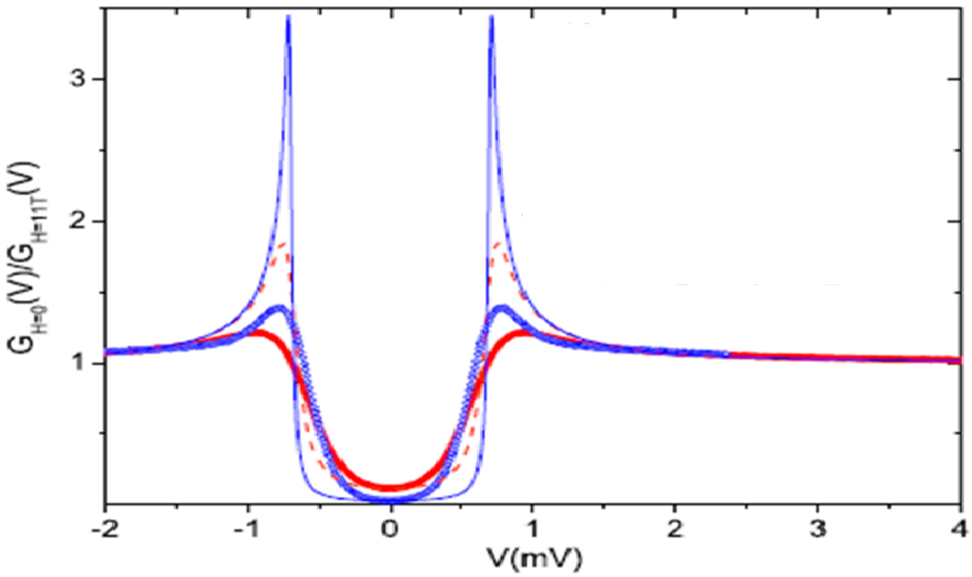

Fig. 1.8 Films of InO_X at both sides of the SIT. The thin lines are the measurements and the thick lines are the best fit to eq. 1.7. The red lines are the insulating film and the blue lines are the superconducting film [18]

Another observation that was observed in samples close to the SIT is that the theoretical BCS temperature dependence of Δ does not fit the measurements [19]. Fig. 1.9 shows measurements of Δ (red line) and Γ (black line) as a function of temperature in two different films of NbN close to the SIT. In contrast to the situation in Fig 1.5, for which at $T = T_c$, $\Delta = 0$, fig. 1.9 shows that at $T = T_c$, $\Delta \neq 0$. This observation is consistent with electronic granularity as well. The energy gap persists even when $T = T_c$. This shows that even above T_c there are signs of superconductivity but there is no coherence across the sample.

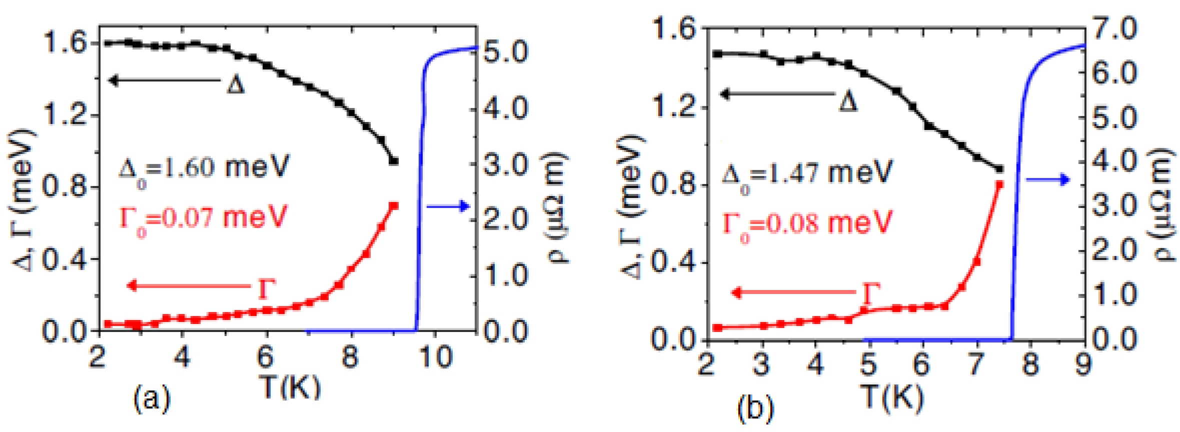

Fig. 1.9: Measurements of $\Delta \& \Gamma$ as a function of temperature in two levels of disorder (a) $T_c = 9.5k$, (b) $T_c = 7.7k$. In both cases it becomes very clear that when $T \rightarrow T_c$, $\Delta \neq 0$ [19].

1.10 Summary

In a clean superconductor there is a good agreement between tunneling measurements and the DOS of the BCS theory. As the system approach the SIT this agreement does not hold anymore. In this work we study films of InO_X close to the SIT at different levels of disorder and in different T_c. We did experiments in attempt to extract information that could give us a new direction for describing the DOS and the energy gap for highly disordered superconductors beyond BCS.

2. Experimental methods

2.1 Sample preparation

SIN junctions were prepared using the following three-stage procedure (see sketch in fig. 2.1):

1. Thermal evaporation of an 100nm thick Aluminum layer.
2. Oxidization of the Aluminum surface in the presence of oxygen, in order to form an insulating tunnel barrier.
3. Electron beam evaporation of a 30nm film of InO_X at different concentrations of oxygen. This layer is used as the disordered superconductor of which the DOS is to be studied.

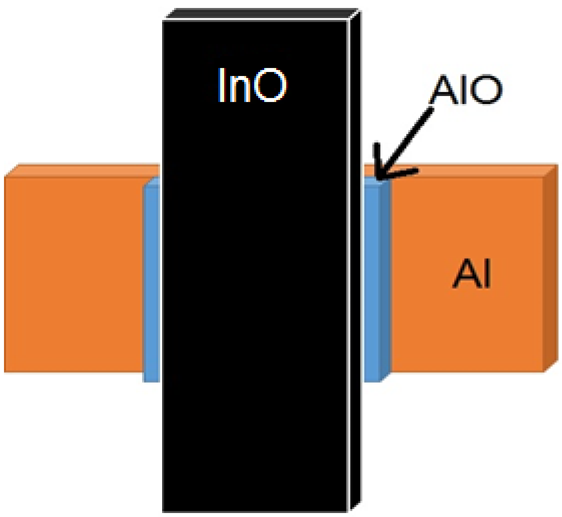

Fig. 2.1: Sketch of our SIN junction – the first layer is aluminum, above it there is aluminum oxide barrier and the last layer is InO_X.

2.2 InO_X layer preparation

Disorder in the InO_X can be controlled in two ways:

1. Changing the oxygen level in the chamber during evaporation: In the evaporation process the chamber is pumped to a base pressure of $\sim 5 * 10^{-7}\text{T}$, after which the oxygen level is controlled by bleeding oxygen into the chamber at pressure of $1 * 10^{-5}\text{T} - 8 * 10^{-5}\text{T}$. By this method we can create different films with different levels of disorder, spanning the entire range of the SIT.

(Increasing oxygen pressure raises the resistance of the sample and pushes it into the insulating state)

2. Annealing - heating the sample to a temperature of $50^{\circ}\mathrm{C}$ for growing periods of time. Every step of annealing reduces the level of disorder: We prepare an insulating film close to the SIT and by the annealing process push it through the SIT. The disorder level is defined by R_{sq} (the resistance per square of the sample at T=6k).

2.3 Measurement setup

Tunneling measurements are performed in a $^{3}\mathrm{He}$ system that has a base temperature of $0.3\mathrm{k}$.
For every sample we performed two simultaneous measurements:

1. Transport (Fig. 2.2): We measured the resistance as a function of temperature, using a quasi 4 probe technique. From this measurement we extract two important parameters: T_c and R_{sq}. These two parameters defined each and every sample; the analyses of the measurements were based on them.

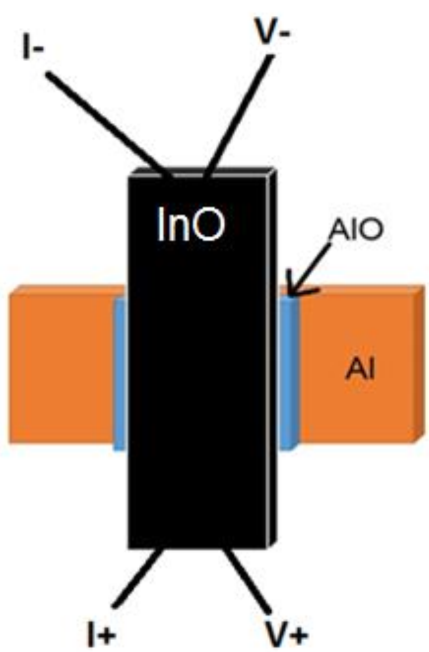

Fig. 2.2: Setup for transport measurements.

2. Tunneling (Fig. 2.3): There are two applicable methods for differential conductance measurements:
   - Applying dc voltage and varying it in small steps ΔV ($V_{n+1} = V_n + \Delta V$). Measuring the current I_n for each applied voltage V_n and calculating the slope: $\frac{dI}{dV} \cong \frac{\Delta I}{\Delta V} = (I_{n+1} - I_n)/(V_{n+1} - V_n)$
   - Using an ac technique; applying a sinusoidal signal superimposed on a dc bias on the sample. Then using a lock-in amplifier to obtain the ac voltage across and the ac current.

Our measurement combined both these methods: We used a current source and a nanovoltmeter as described in fig. 2.3.

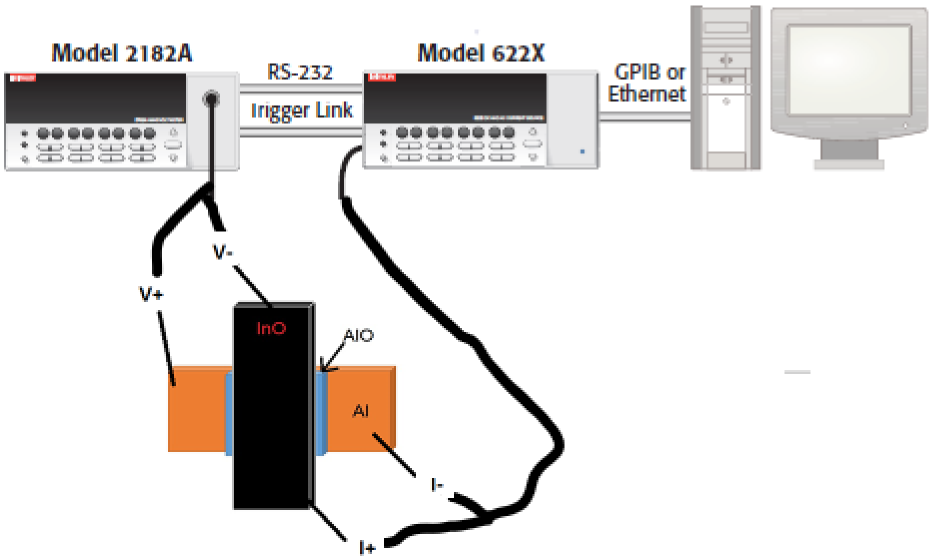

Fig. 2.3: A setup of the tunneling differential conductance measurement: We apply current to the sample by a Keithley 6221 current source and measure the voltage with a Keithley 2182A nanovoltmeter.

The method of the measurement is sketched in fig. 2.4: The current sources (Keithley 6221) combine the dc and ac components into one source (Fig. 2.4(a)) by adding an alternating current to a linear staircase sweep. The amplitude of the alternating portion of the current is the differential current, dI. The voltage is measured by the nanovoltmeter (Fig. 2.4(b)) for each step of the sweep measured the voltage (V_1, V_2, V_3 …) and calculating the dV is very similar to the first method that calculates differential conductance ($dV = [(V_1 - V_2) + (V_3 - V_2)]/4$).

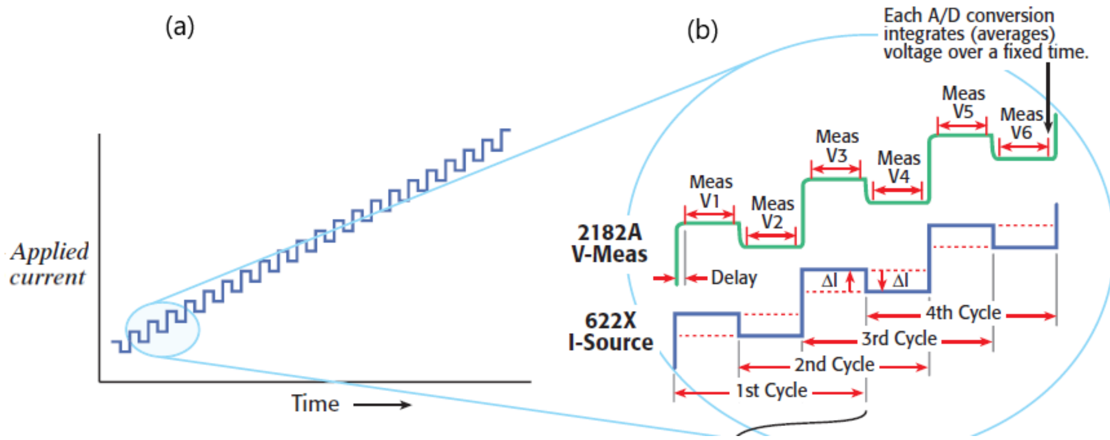

Fig. 2.4: (a) plot of the applied current as a function of time. (b) a close look on the applied current and measured voltage.

Since for tunneling measurements we a real insulating tunnel barrier, the resistance of the junction (R_j) must be much larger than the resistance of the InOx film, otherwise the measurements will be meaningless (the InOx will not be an equi-potential electrode making the tunneling experiment useless). In our experiment we made sure that R_j was at least two orders of magnitude larger then R_{InO}.

3. Results & discussion

3.1 Transport measurements

In our experiment we change the properties of InO_X films using two methods: (1) Annealing (2) changing the oxygen level during evaporation. The former changes the disorder and the latter changes the density of the electrons. Therefore we present their resistance versus temperature (RT) measurements in two different graphs: Fig. 3.1a shows the transport measurements of a film in which resistance was varied by annealing and fig. 3.1b shows the transport measurements of a set of samples with different oxygen pressure. It is seen that both methods influence R_{sq} and T_c in correlated way. We note that there is some deviation in the last annealing stage, seen in fig. 3.1, probably due to some artifact that occurred during the last stage preparation.

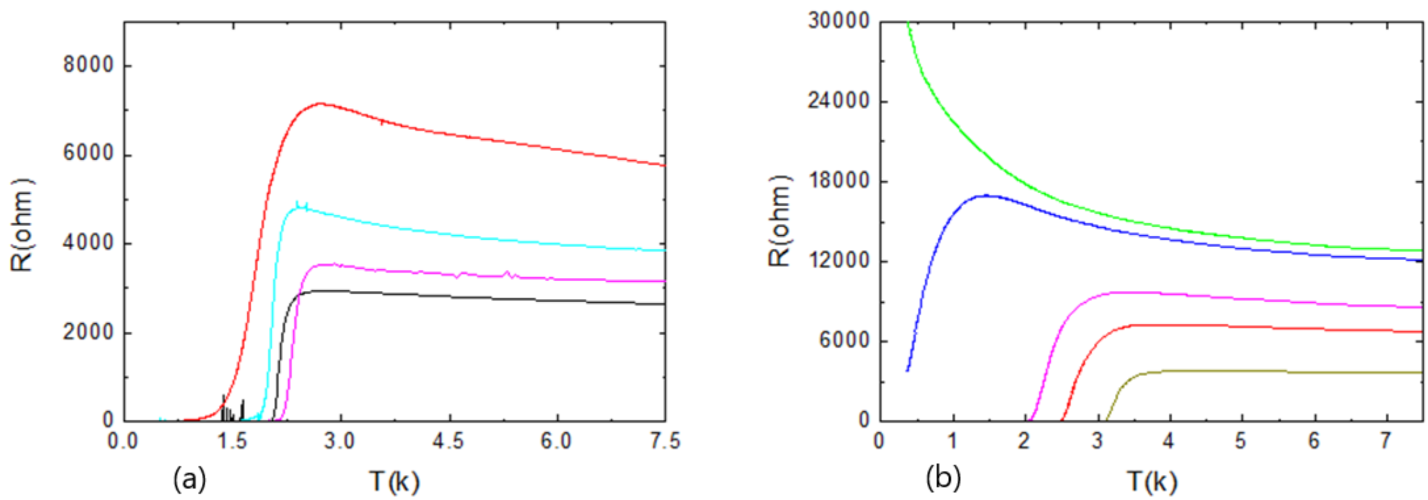

Fig. 3.1: Resistance per square versus T of our samples prepared by; (a) different annealing stages, (b) different oxygen pressure during evaporating.

3.2 Tunneling measurements

We measured 13 samples at different levels of disorder. For each sample, we performed tunneling measurements across the junction at different temperatures. In fig. 3.2 we present tunneling measurements of two typical samples, one taken from fig. 3.1a and the other from fig. 3.2b. It is seen that as the temperature rises, the coherence peaks get smaller. On the other hand, the energy scale of the gap does not change even when the temperature rises above T_c. Similar behavior is seen for all measured samples.

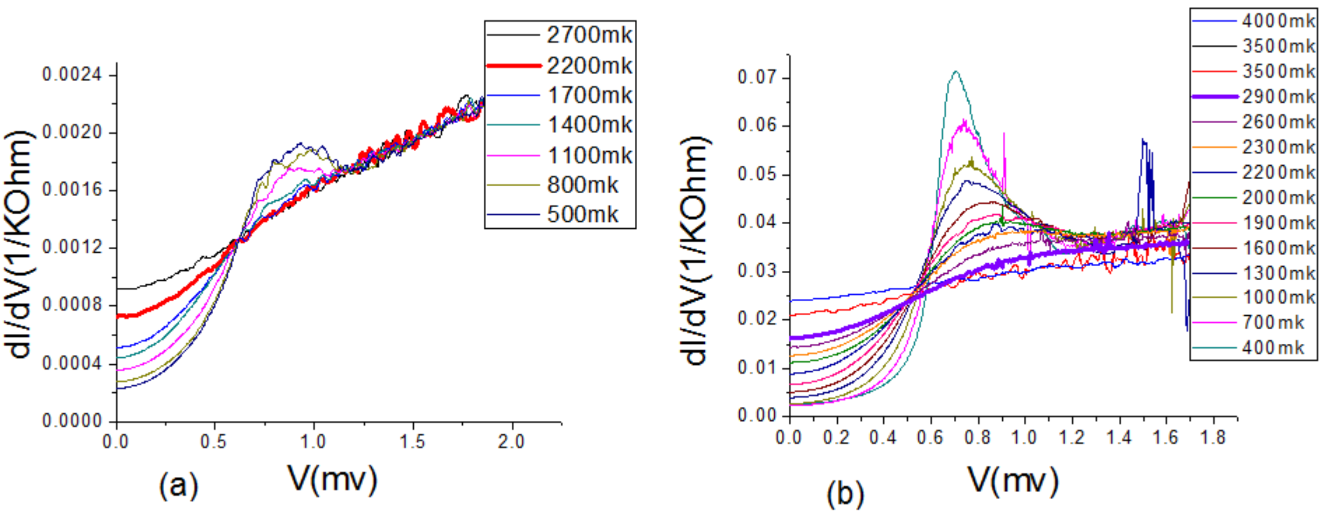

Fig. 3.2: $\frac{dI}{dV}$ as a function of V for two typical samples at different temperatures. The heavy lines are the measurement at T_c.

3.3 Extracting the superconductor DOS

Our results do not directly provide the DOS of the superconductor because there are two contributions to the experimental curves, the DOS of the metallic state and the DOS of the superconducting state of the InO_x film. As mentioned in the introduction, tunneling measurements and the DOS of the superconductor deduced from them are based on the constant value of the DOS of the metallic state near E_f, which is valid in the case of ordered metallic films. When the metal is disordered, the DOS is suppressed near E_f due to electron-electron interaction. This is described by the Altsuler & Aronov expression [20].

$$\frac{dI}{dV}/\frac{dI}{dV}(\infty) = 1 - \frac{1}{4\pi^2\hbar g}\ln\frac{2\kappa b}{k}\ln\frac{\varepsilon\tau}{\hbar} \tag{3.1}$$

Where $\mathcal{E} = \max(V, T)$, g is the dimensionless conductance, κ is the inverse screening length, τ is the inelastic relaxation time, k is the dielectric function, and b is the barrier thickness. To take this effect in account we fit our data to a simplified expression that contributes to the differential conductance measurements:

$$\frac{dI}{dV} = \frac{dI}{dV}(\infty) * (1 - A_1 \ln(\varepsilon * A_2)) \tag{3.2}$$

This fit is performed for the results at high energies $V > \Delta$ and extrapolated to $V = 0$. We then normalize the measurements by dividing the raw data by the extracted $\frac{dI}{dV}$ of the normal state (eq. 3.2). The results for the samples of fig. 3.2 are shown in fig. 3.3.

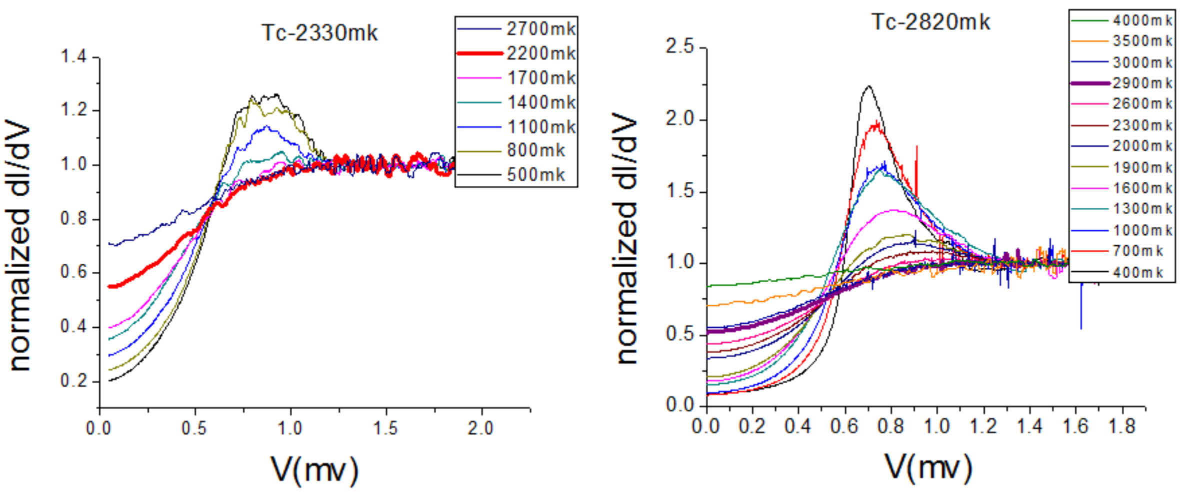

Fig. 3.3: Normalized $\frac{dI}{dV} - V$ of the samples from Fig. 3.2. The heavy lines are the measurements at T_c.

These results demonstrate even more clearly that the energy gap (Δ) still exists above T_C.

Fig. 3.4 shows attempts to fit our results to eq.1.7 (BCS theory) for two temperatures. It is clear that the fits is very close to BCS, as indeed was observed in the past for samples close to the SIT (see introduction).

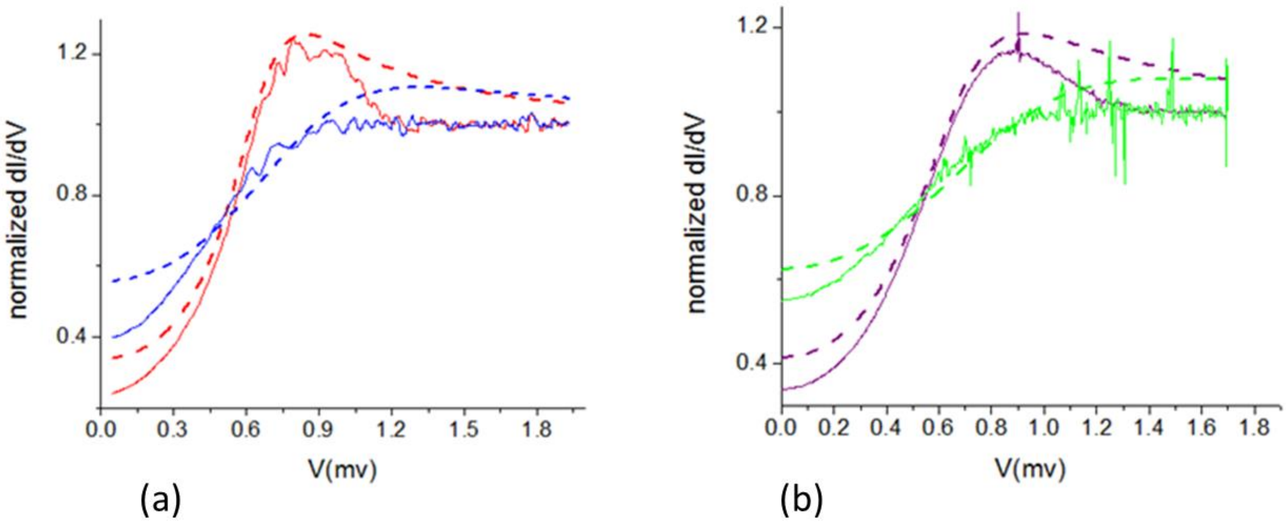

Fig. 3.4: The best fit to eq. (1.7) at two different temperatures for the two samples of fig. 3.3: (a) The fits for the sample from fig. 3.3a; Red lines denote $T = 1.7k$, blue lines denote $T = 0.8k$. (b) The fits for the sample from fig. 3.3b; purple lines denote $T = 1k$, green lines denote $T = 2k$. Solid lines are experiment results, dashed lines are fits to BCS.

3.4 A new approach

Dentelski, et al [21] suggest a new approach for tunneling experiments in disordered superconductors. In this model Δ is not a constant but a bosonic field that changes in space and time {Δ(r,t)} with a finite correlation length. They show that one can express Δ as a function of long range (LR) and short range (SR) correlations: Where SR are correlations between neighboring grains (SR represent the difference between BCS and disorder superconductor) and LR are correlations throughout the entire sample ($\mathrm{LR} \propto \Delta$). In this model one can present two parameters, S_0 and S_1 so that: $\mathrm{SR} \propto -\mathrm{iE} * S_1$ and $LR \propto (S_0)^2$. Therefore Δ can be presented as a sum of LR+SR in the following way.

$$\Delta^2 \cong (\mathrm{S}_0)^2 - \mathrm{iE} * \mathrm{S}_1 \tag{3.3}$$

Inserting Δ into eq. (1.7) gives:

$$\frac{\mathrm{dI}}{\mathrm{dV}} = \left|\mathrm{Re}\left[\frac{\mathrm{E}-\mathrm{i}\Gamma}{\sqrt{(\mathrm{E}-\mathrm{i}\Gamma)^2+(\mathrm{S}_0)^2-\mathrm{iES}_1}}\right]\right| \tag{3.4}$$

Fig. 3.5 shows the fits of our results to eq. 3.4. Clearly this approximation yields much better fit than eq.1.7 at high energies

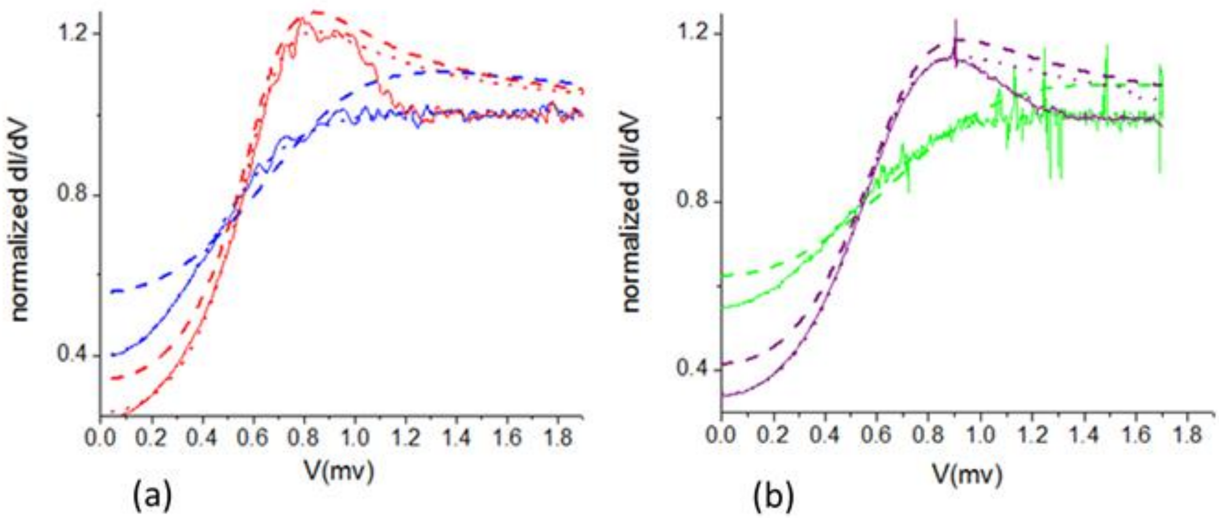

Fig. 3.5: The best fit to eq. (1.7) and eq. (3.4) at two different temperatures for two samples: (a) The sample from fig. 3.4a; Red lines denote $T = 1.7k$, blue lines denote $T = 0.8k$. (b) The sample from fig. 3.4b; Purple lines denote $T = 1k$, green lines denote $T = 2k$. Solid lines are experiment results, dashed lines are fits to BCS and dotted lines are fits to eq. (3.4).

3.5 The fitting parameters

The results presented in fig. 3.5 involve three fitting parameters: S_0 , S_1 and Γ:

- S_0- In the limit of clean samples and at long distance $\Delta \sim S_0$.
- S_1- Is a measure of the difference between disordered superconductors and BCS superconductors.
- Γ- Is same as in eq. 1.7: A phenomenological smearing parameter that takes into account all the thermal and external RF noises;$1/\tau$ where τ is the electron lifetime.

For every plot of tunneling measurements we found the best fit to eq. 3.4 and recorded these fitting parameters.

Fig. 3.6 shows S_0 , S_1 and Γ as functions of T/T_c for representative films. It is seen that S_0 is almost constant even when T is much larger than T_c. This it is not consistent with BCS theory because according to eq. 1.3 at $T = T_c$, $\Delta = 0$. Our results are consistent with the bosonic model for SIT that predicts the presence of superconductivity at $T > T_c$.

S_1 shows a maximum at $0.8T_c$. This may be due to the fact that S_1 is a measure of the difference between disordered superconductors and BCS superconductors. This difference is reflected mostly near T_c, because according to the BCS all the superconducting properties should disappear at $T = T_c$. In films near the SIT the coherence peaks is vanished at T_c but the energy gap still exist above T_c. Therefore, near T_c, S_1 has maximal value. When T rises the superconducting properties disappear, therefore, the value of S_1 drops.

The value of Γ rises sharply with T as we get approach T_c: This is understood by the fact and the noises rises when the system approaches T_c.

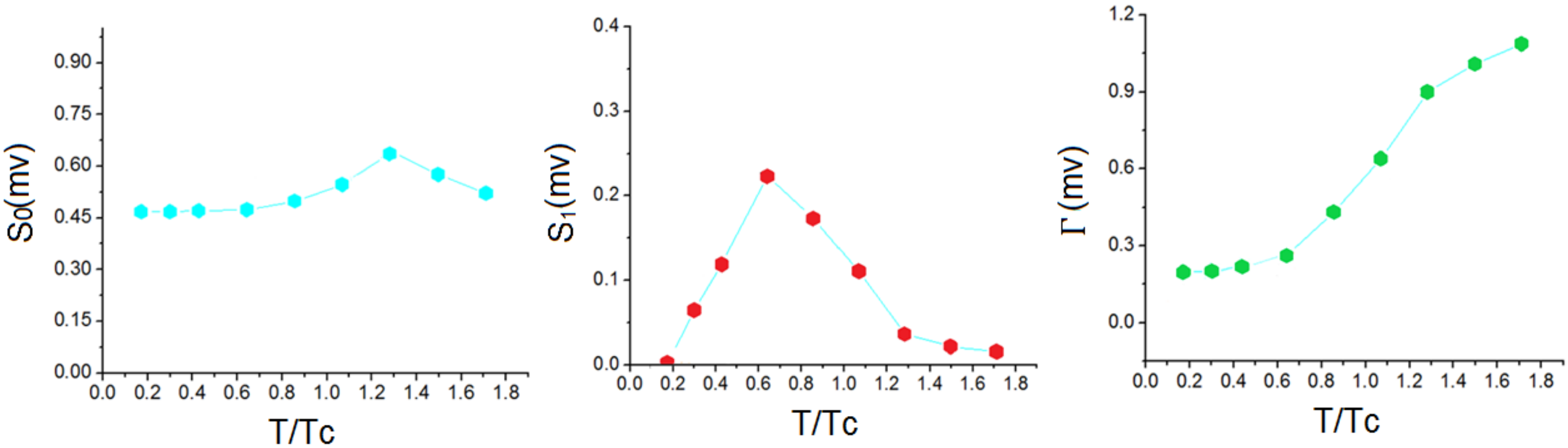

Fig. 3.6: S_0 (a), S_1 (b) and, Γ (c) as a function of T/T_c.

3.6 S_0 and S_1 across the SIT

Fig. 3.7 shows the value of S_0 , S_1 at $T = 0.5k$ as a function of R_{sq}. Fig. 3.7a shows that as R_{sq} rises the value of S_0 in both sets of samples have a small drop, but when the sample enters the insulating phase we observe a rise in S_0: It is resemble that S_0 will drop as the disorder rises because as the system approaches the SIT the superconductivity properties starts to disappear. The jump in the insulating phase is need to be checked more carefully (we have gust one measurement).

Fig. 3.7b shows that S_1 had increases dramatically as the system approaches the insulating phase. This is consistence with the understanding that fluctuations in Δ increase close to the SIT. We note that, even at low values of R_{sq} $S_1 \neq 0$. This means that even our most ordered films are far from being BCS superconductors.

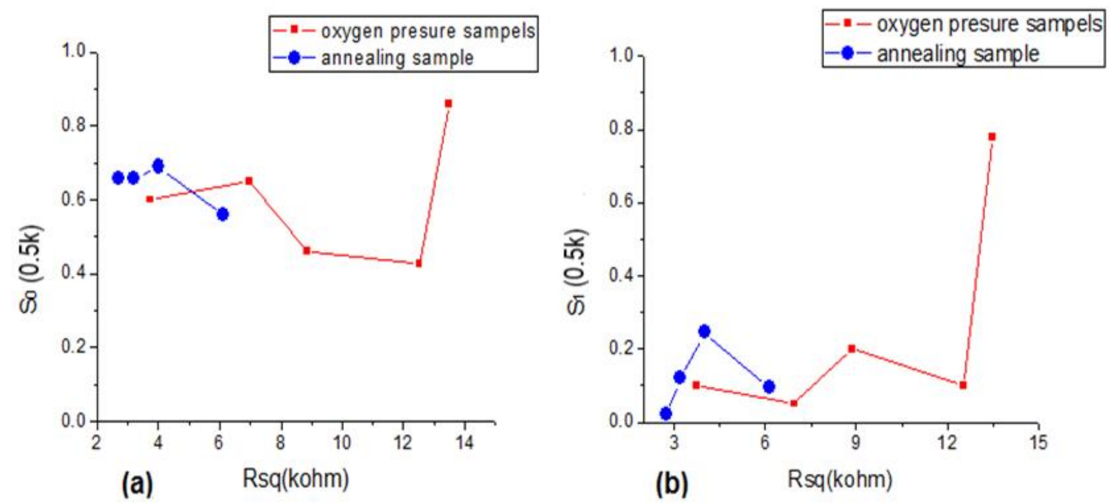

Fig. 3.7: S_0 (a) and S_1 (b) at $T = 0.5k$ as a function of R_{sq}.

Finally we define the temperature range of S_1, WS_1 ,by extracting the full width of S_1 at half value (WS_1) as demonstrated in fig. 3.8b. Fig 3.8a shows WS_1 as a function of R_{sq}: It illustrates that WS_1 rises with R_{sq}. We can conclude that the coherence peaks drop in lager spectrum of temperatures as R_{sq} is growing.

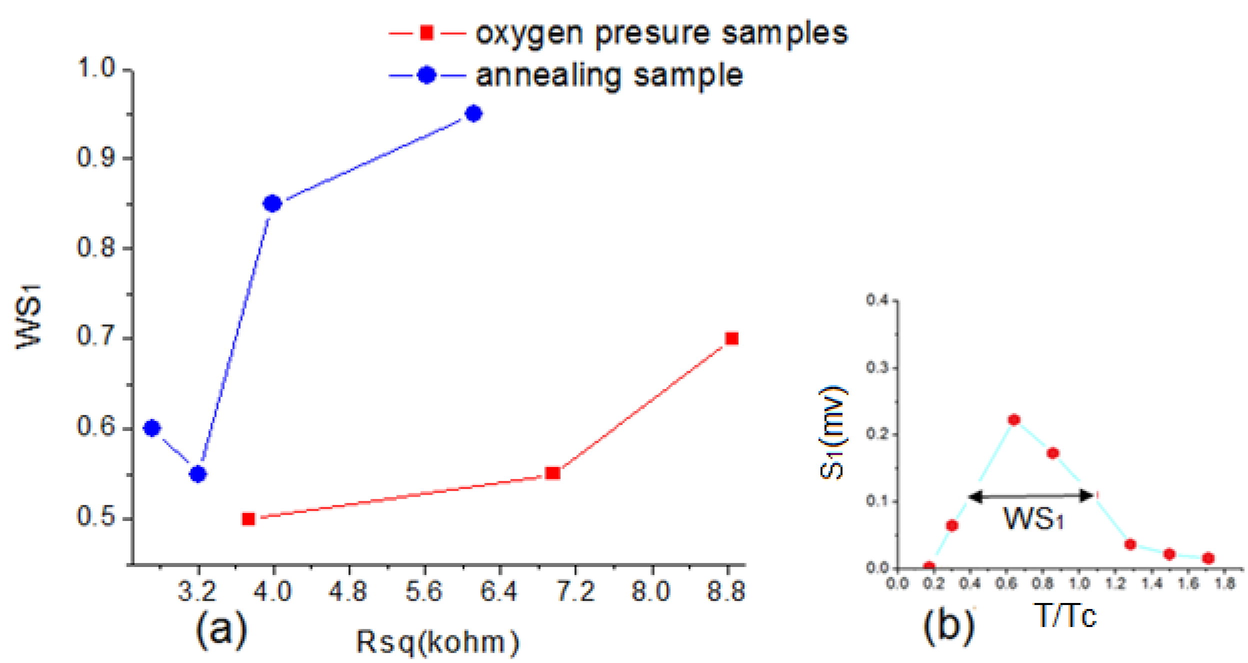

Fig. 3.8:(a) WS_1 as a function of R_{sq}.(b) WS_1 in typical sample

.

4. Conclusions

- InO_X films belong to a unique type of systems that undergo the SIT, and exhibit interesting behavior in the region of the transition: Although the structure of the film is morphologically homogeneous it shows signs typical of granular systems. This happens due to the presence of emergent electronic granularity.
- While the DOS for an ordered superconductor is described by the BCS theory, the measurements of the DOS of InO_X films close to the SIT do not fit the BCS theory very well. Moreover, unlike BCS superconductors in which the energy gap approach zero when $T = T_c$, in InO_X films Δ exists even above T_c. In addition, the behavior of the coherence peaks of these films do not fit BCS. Therefore, a new theory is suggested in which the energy gap is not a constant but a bosonic field , $\Delta(\mathrm{r}, \mathrm{t})$, that depends on long range (LR) and short range (SR) correlations.
- The fits of our results to the new theory are much better than the fits to the BCS theory.
- The fitting procedure produces three fitting parameters, S_0, S_1 and Γ for each film. We examined the change of the parameters as a function of $\mathrm{T}/\mathrm{T_c}$:
    1. S_0 – Almost does not change as the temperature rises: Long-range correlations that represent the energy gap, still exist above the critical temperature. This is consistent with the bosonic model for SIT that predicts the presence of superconductivity at $\mathrm{T} > \mathrm{T_c}$.
    2. S_1- Shows a maximum at $0.8T_c$. This may be due to the fact that S_1 is a measure to the difference between disordered superconductors to a BCS superconductor. Which is maximal at $T \cong T_c$.
    3. Γ- Rises sharply with T as we get approach T_c: This is understood by the fact and the noises rises when the system approaches T_c.
- Investigation of S_0 and S_1 as a function of R_{sq} at $T = 0.5k$ yields the following conclusions:
    1. S_0 – Have a small drop when R_{sq} rises, until the film enters the insulating phase where the value of S_0 rises: It is resemble that S_0 will drop as the disorder rises because as the system approaches the SIT the superconductivity properties starts to disappear. The jump in the insulating phase is need to be checked more carefully (we have just one measurement).
    2. S_1- Had increases dramatically as the system approaches the insulating phase. This is consistence with the understanding that fluctuations in Δ increase close to the SIT.

4. References

[1] R. H. Mckenzie, Q. Wang, and H. T. Quan, REPORTS Prog. Phys. **66**, 2069 (2003).

[2] S. Sachdev, Cambridge Univ. Press (1999).

[3] J. Bardeen, L. N. Cooper, and J. R. Schrieffer, Phys. Rev. **108**, 1175 (1957).

[4] P. W. ANDERSON, J. Phys. Chem. Solids **11**, 26 (1959).

[5] D. B. Haviland, Y. Liu, and A. M. Goldman, Phys. Rev. Lett. **62**, 2180 (1989).

[6] N. Markovic, C. Christiansen, and A. M. Goldman, Phys. Rev. Lett. **81**, 5217 (1998).

[7] B. Sacépé, C. Chapelier, T. I. Baturina, V. M. Vinokur, M. R. Baklanov, and M. Sanquer, Phys. Rev. Lett. **101**, 1 (2008).

[8] S. Poran, A. Auerbach, N. Dupuis, A. Frydman, and O. Bourgeois, Nat. Commun. **8**, 1 (2017).

[9] H. Aubin, A. Pourret, K. Behnia, J. Lesueur, and L. Dumoulin, Phys. Rev. B **78**, 1 (2008).

[10] T. I. Baturina, D. R. Islamov, J. Bentner, C. Strunk, M. R. Baklanov, and A. Satta, J. Exp. Theor. Phys. Lett. **79**, 337 (2004).

[11] W. T. Herrera, I. S. Dinola, M. A. Continentino, H. Micklitz, Y. T. Xing, and M. B. Fontes, Eur. Phys. J. B **86**, 2 (2013).

[12] A. Frydman, Phys. c **391**, 189 (2003).

[13] A. M. Finkel'shtein, JETP Lett. **45**, 46 (1987).

[14] P. W. Anderson, Phys. Rev. **109**, 1492 (1958).

[15] M. P. A. Fisher, P. B. Weichman, G. Grinstein, and D. S. Fisher, Phys. Rev. B **40**, 546 (1989).

[16] B. B. Ridge, I. L. Dubuque, I. A. Madison, W. I. New, Y. San, and F. St, Concepts Mod. Phys. **6**, (2008).

[17] R. C. Dynes, J. P. Garno, G. B. Hertel, and T. P. Orlando, Phys. Rev. Lett. **53**, 2437 (1984).

[18] D. Sherman, G. Kopnov, D. Shahar, and A. Frydman, Phys. Rev. Lett. **108**, 25 (2012).

[19] S. P. Chockalingam, M. Chand, A. Kamlapure, J. Jesudasan, A. Mishra, V. Tripathi, and P. Raychaudhuri, Phys. Rev. B. **79**, 1 (2009).

[20] B. L. Altshuler, A.G. Aronov, M. E. Gershenson, and Yu.V. Sharvin, Sci. Rev., Sect. A **9**, 223 (1987).

[21] D. Dentelski, A. Frydman, E. Shimshoni, and E. G. D. Torre, arXiv:1706.06601 (2017).

תקציר

מעבר על מוליך-מבודד (SIT) בשכבות דקות היא תופעה שנמצאת בחזית המחקר בימינו. מעבר זה הוא דוגמא קלאסית למעבר פאזה קוונטי שבו המערכת עוברת מהפאזה המבודדת לפאזה העל-מוליכה ב $T = 0$. מרבית המחקרים בנושא ה-SIT מתמקדים באזור הקוונטי הקריטי, מכיוון שבאזור זה התנהגות המערכת היא לא טריוויאלית. עקב כך, נושא זה גרר מאמצי מחקר גדולים, בתחום הניסיוני והתיאורטי, כשמרבית הפיזיקה בתחום הנ"ל עדיין לא מובנת היטב.

אחד המודלים שהוצע להסביר את האפיון במערכת הזאת (SIT) הוא מודל הגרנולריות האלקטרונית, שמתאר מערכת שמראה התנהגות גרנולרית למרות שהיא אחידה מבחינה מיבנית. ניסויים הראו שהגרנולריות נובעת מזה שיש איים על מוליכים בתוך שיכבה מבודדת. שכבות של InO_x (אינדיום אוקסיד) שעוברות את ה SIT, הם דוגמא אחת למערכת הייחודית הזאת.

דרך טובה לאפיין כל על-מוליך היא על ידי ביצוע ניסויי מנהור למדידת צפיפות המצבים, מה שיתן לנו מידע על פער האנרגיה, Δ , של העל-מוליך. מדידות אלו שבוצעו בעבר בעל-מוליכים עם אי סדר גבוה גילו נוכחות של על מוליכות בפאזה המבודדת.

בעבודה זאת מדדנו את צפיפות המצבים בשכבות של InO_x קרוב למעבר על מוליך –מבודד ברמות שונות של אי סדר ובמגוון טמפרטורות. בעל-מוליכים נקיים מדידת צפיפות המצבים מראה התאמה טובה לביטוי הידוע מתאורית ה- BCS. לעומת זאת, צפיפות המצבים בעל מוליכים שקרובים לSIT לא מראה התאמה טובה ל BCS. בייחוד המקסימום בקצוות של פער האנרגיה (coherence peaks) שהופחת במידה ניכרת.

השתמשנו בגישה חדשה כדי לנתח את מדידות המנהור. גישה זאת לוקחת בחשבון את המבנה האלקטרוני (גרנולריות האלקטרונית) שבו Δ לא קבוע אלה שדה בוזוני עם פלקטואציות במרחב ובזמן $\{\Delta(r,t)\}$.ניתן לבטא את Δ כקומבינציה של השפעות של קורלציות קצרות וארוכות טווח: ניתחנו את התוצאות שלנו בעזרת התאוריה הזאת ומצאנו שההתאמות לתיאוריה החדשה היו הרבה יותר טובות מההתאמות ל BCS ,כאשר הוספנו רק פרמטר התאמה אחד.

המסקנות העיקריות מניתוח התוצאות הם:

1. Δ לא משתנה יחד עם אי סדר וטמפרטורה. בנוסף לכך, הוא נשאר קבוע אפילו מעל T_c וגם בתוך המבודד.
2. תאוריית ה BCS לא מספיקה כדי לתאר את הפיזיקה באזור ה SIT. אנו מראים שצריך לקחת בחשבון פלקטואציות בפרמטר הסדר כדי להבין את הפיזיקה.
3. הצורך בגישה החדשה גובר ככל שהמערכת מתקרבת ל SIT.

עבודה זו נעשתה בהדרכתו של

פרופ' אביעד פרידמן

מן המחלקה לפיסיקה של אוניברסיטת בר-אילן

אוניברסיטת בר אילן

המחלקה לפיסיקה

מדידות מנהור בדגמים לא מסודרים ליד מעבר על מוליך-מבודד.

אוריה אייזנברג

מוגש כחלק מהדרישות לשם קבלת תואר מוסמך

במחלקה לפיזיקה של אוניברסיטת בר אילן

תשע"ח רמת-גן, ישראל

אוניברסיטת בר אילן

המחלקה לפיסיקה

מדידות מנהור בדגמים לא מסודרים ליד מעבר על מוליך-מבודד.

אוריה אייזנברג

מוגש כחלק מהדרישות לשם קבלת תואר מוסמך

במחלקה לפיזיקה של אוניברסיטת בר אילן

תשע"ח רמת-גן, ישראל